Partial Coherence

Offner catoptric system

As an example of the effects of coherence on imaging, we will use a two-mirror, monocentric system of the type originally designed by Offner (U.S. Patent 3,748,015). For an object placed in the plane containing the common centers of curvature, the imagery is 1:1 and all of the Seidel aberrations are zero. This type of system has been widely used in photolithographic systems. The radius of curvature of the large, concave mirror is twice the radius of curvature of the small, convex mirror. The aperture stop is located at the small mirror so this system is essentially telecentric. We start with the following system and use the mercury *i*-line at 0.365 µm.

```
*LENS DATA
Offner Catoptric System
 SRF      RADIUS         THICKNESS    APERTURE RADIUS        GLASS   SPE    NOTE
  0         --          100.000000     20.000000               AIR

  1    -100.000000     -50.000000      38.000000        REFL_HATCH

  2     -50.000000      50.000000      10.000000 A      REFL_HATCH

  3    -100.000000    -100.000000      38.000000           REFLECT

  4         --             --          20.000000 S

*PARAXIAL SETUP OF LENS
APERTURE
   Object num. aperture:      0.170000    F-number:                    --
FIELD
   Gaussian image height:   -20.000000    Chief ray ims height:     20.000000

*WAVELENGTHS
CURRENT   WV1/WW1
   1     0.365010
```

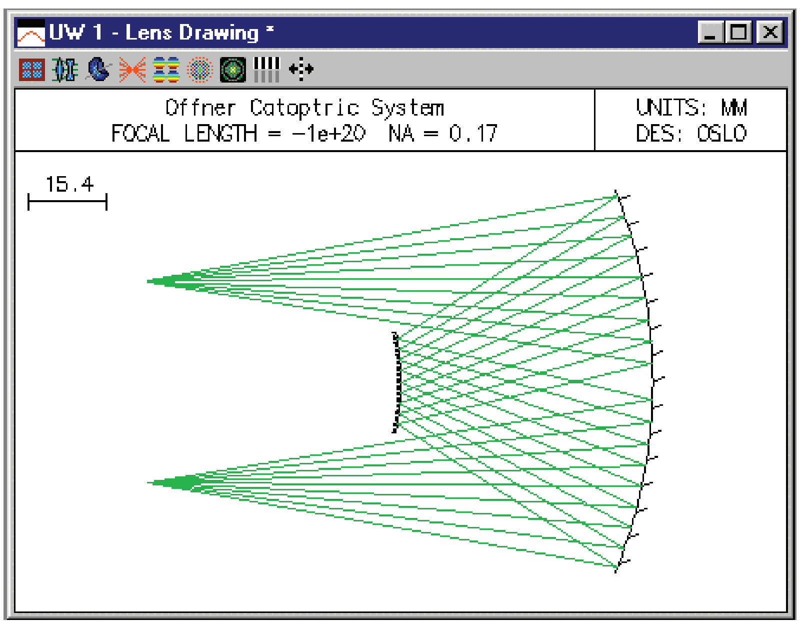

Obviously, because of the location of the secondary mirror, this system is only used with off-axis object points. In this nominal design, the performance is limited by fifth-order astigmatism. If the separation of the mirrors is changed slightly, a small amount of third-order astigmatism can be introduced and the third-order and fifth-order astigmatism can be made to balance at one object height. Thus, the resulting system has a single (object) zone of good correction and can be used as a "ring-field" system (i.e., a field of view in the shape of a section of an annulus or ring). In order to make this modification to the lens, we first enter minus thickness pickups for surfaces 2 and 3, in order to maintain the desired system geometry. Also, we make thicknesses 0 and 1 variable.

```
*LENS DATA
Offner Catoptric System
 SRF      RADIUS      THICKNESS   APERTURE RADIUS       GLASS  SPE   NOTE
  0         --       100.000000 V   20.000000            AIR

  1   -100.000000    -50.000000 V   38.000000      REFL_HATCH

  2    -50.000000     50.000000 P   10.000000 A    REFL_HATCH

  3   -100.000000   -100.000000 P   38.000000         REFLECT

  4         --           --         20.000000 S

*PICKUPS
  2     THM    1
  3     THM    0

*VARIABLES
 VB   SN  CF  TYP        MIN         MAX        DAMPING      INCR        VALUE
V 1    0   -  TH      0.100000  1.0000e+04    1.000000    0.001725   100.000000
V 2    1   -  TH   -1.0000e+04   -0.100000    1.000000    0.001725   -50.000000
```

We could do the optimization in several ways, but the simplest is probably to use OSLO's automatic error function generation to create an error function that measures the RMS OPD at the selected object point. We choose to balance the astigmatism at a fractional object height of 0.95 (i.e., an object height of –19.0 mm). With this field point, the result of using the error function generator is

```
*RAYSET
FPT       FBY/FY1       FBX/FY2       FBZ/FX1       YRF/FX2       XRF/WGT
F 1       0.950000         --            --            --            --
         -1.000000      1.000000     -1.000000      1.000000      1.000000
RAY         TYPE          FY            FX           WGT
R 1       Ordinary         --            --         0.041667
R 2       Ordinary      0.525731         --         0.208333
R 3       Ordinary      0.262866      0.455296      0.208333
R 4       Ordinary     -0.262866      0.455296      0.208333
R 5       Ordinary     -0.525731         --         0.208333
R 6       Ordinary      0.850651         --         0.208333
R 7       Ordinary      0.425325      0.736685      0.208333
R 8       Ordinary     -0.425325      0.736685      0.208333
R 9       Ordinary     -0.850651         --         0.208333
R 10      Ordinary      1.000000         --         0.041667
R 11      Ordinary      0.500000      0.866025      0.041667
R 12      Ordinary     -0.500000      0.866025      0.041667
R 13      Ordinary     -1.000000         --         0.041667

*OPERANDS
 OP    DEFINITION                  MODE     WGT      NAME          VALUE   %CNTRB
O 15   "RMS"                         M    0.500000 Orms1         2.771379 100.00
MIN ERROR:     2.771379
```

After a few iterations, the resulting system is as given below.

```
*LENS DATA
Offner Catoptric System
 SRF      RADIUS       THICKNESS   APERTURE RADIUS       GLASS SPE   NOTE
  0         --        100.870668 V   20.000000            AIR

  1    -100.000000    -49.078862 V   38.000000       REFL_HATCH

  2     -50.000000     49.078862 P   10.000000 A     REFL_HATCH

  3    -100.000000   -100.870668 P   38.000000          REFLECT

  4         --            --         20.023377 S
```

The field curves indicate that the desired astigmatism balance has been achieved.

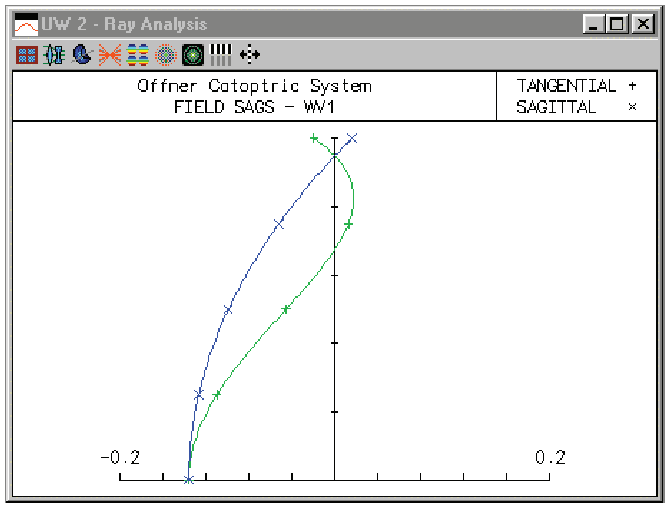

The numerical aperture of this lens is 0.17, so the diameter of the Airy disk is 1.22 λ_0 / *NA* = 1.22 (0.365 μm) / 0.17 = 2.62 μm. Thus a perfect image bar width of 7 μm should be easily resolved and be suitable to demonstrate coherence effects. The optimized lens is essentially diffraction limited at the design field of 0.95, so the resulting image at this object point will be indicative of the effects of coherence and diffraction.

In the partial coherence operating conditions, we define the ideal image to consist of two bars, each of width 7 μm and separated by 14 μm.

```
*OPERATING CONDITIONS: PARTIAL COHERENCE
   Effective source rad.:        --       Inner annular radius:        --
   X shift of source:            --       Y shift of source:           --
   X 1/e^2 of source:            --       Y 1/e^2 of source:           --
   Number of points in image:      64     Number of clear bars in image:    2
   Width of clear bar:         0.007000   Period of clear bars:      0.014000
   Irrad. between bars:          --       Phase between bars:          --
   Background irradiance:        --
   Normalization:    Object irradiance    Use equal image space incrmnts.:Off
```

We will examine the image as we change the illumination from a point effective source (i.e., fully coherent; $\sigma = 0$) to an effective source that completely fills the entrance pupil ($\sigma = 1$). We also examine the incoherent limit.

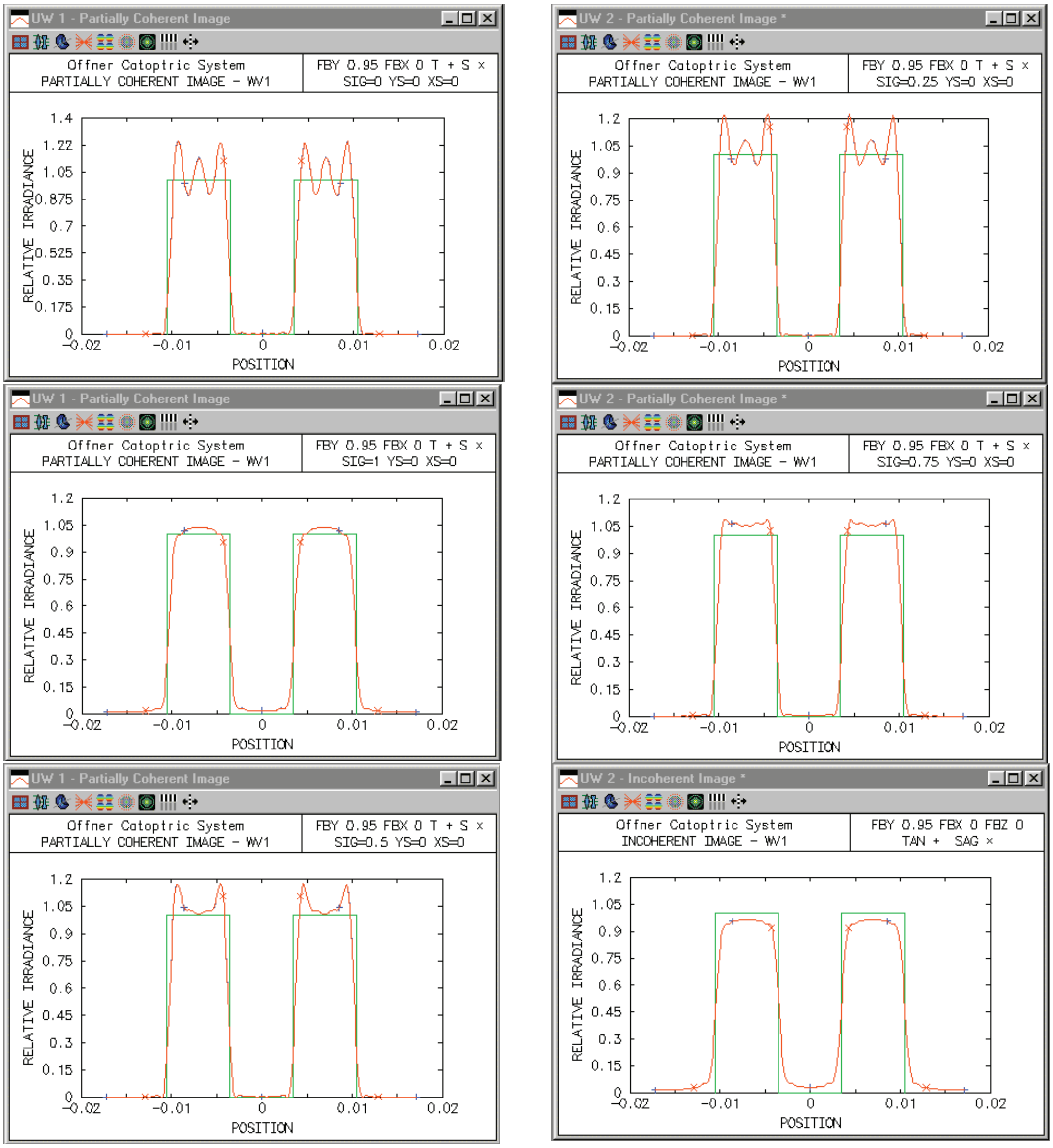
UW 1 - Partially Coherent Image
Offner Catoptric System
PARTIALLY COHERENT IMAGE - WV1
FBY 0.95 FBX 0 T + S x
SIG=0 YS=0 XS=0
RELATIVE IRRADIANCE
POSITION
UW 2 - Partially Coherent Image *
Offner Catoptric System
PARTIALLY COHERENT IMAGE - WV1
FBY 0.95 FBX 0 T + S x
SIG=0.25 YS=0 XS=0
RELATIVE IRRADIANCE
POSITION
UW 1 - Partially Coherent Image
Offner Catoptric System
PARTIALLY COHERENT IMAGE - WV1
FBY 0.95 FBX 0 T + S x
SIG=1 YS=0 XS=0
RELATIVE IRRADIANCE
POSITION
UW 2 - Partially Coherent Image *
Offner Catoptric System
PARTIALLY COHERENT IMAGE - WV1
FBY 0.95 FBX 0 T + S x
SIG=0.75 YS=0 XS=0
RELATIVE IRRADIANCE
POSITION
UW 1 - Partially Coherent Image
Offner Catoptric System
PARTIALLY COHERENT IMAGE - WV1
FBY 0.95 FBX 0 T + S x
SIG=0.5 YS=0 XS=0
RELATIVE IRRADIANCE
POSITION
UW 2 - Incoherent Image *
Offner Catoptric System
INCOHERENT IMAGE - WV1
FBY 0.95 FBX 0 FBZ 0
TAN + SAG x
RELATIVE IRRADIANCE
POSITION

We see that as the coherence decreases, the "interference-like" ringing of the edges of image decreases. In photolithography, it is usually the slopes of the edges of the image that are of interest; higher slopes lead to smaller changes in linewidth with changes in exposure. As the above figures indicate, in addition to controlling the aberrations of the imaging lens, the illumination coherence (i.e., the value of σ) must be considered when calculating overall system performance. If we look at the structure of the image for a fractional object height of 0.8 (i.e., an image height of 16 mm), we see the effects of the astigmatism on the coherent and incoherent images.

- Coherent

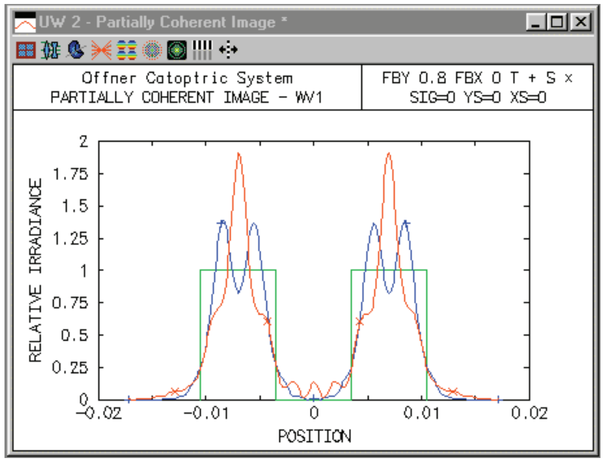

- Incoherent

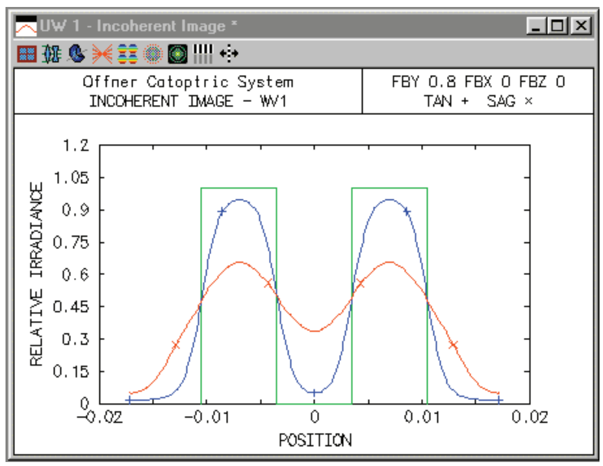

Talbot effect

A striking example of the influence of coherence upon imaging is provided by the *Talbot effect*. If a coherent field has a periodic spatial amplitude distribution, the propagating field exhibits self-imaging, i.e., the image replicates itself at prescribed longitudinal distances. Compare this to the familiar case of incoherent illumination, where, in general, the modulation of an image decreases as we move the observation plane longitudinally from focus.

As a simple demonstration, we start with a 100 mm focal length perfect lens of numerical aperture 0.05 and monochromatic illumination of wavelength 0.5 µm.

Gen | Setup | Wavelength | Field Points | Variables | Draw Off | Group | Notes

Lens: Talbot Effect Defocus = 0 | Zoom 1 of 1 | Efl 100.000000

Ent beam radius 5.000000 | Field angle 5.7296e-05 | Primary wavln 0.500000

SRF	RADIUS	THICKNESS	APERTURE RADIUS	GLASS	SPECIAL
OBJ	0.000000	1.0000e+20	1.0000e+14	AIR	
AST	ELEMENT GRP	0.000000	5.000000 AS	AIR	F
2	PERFECT	100.000000 S	5.000000 S	AIR	NL
IMS	0.000000	0.000000	1.0000e-04 S		

We will use a perfect image that consists of an infinite pattern of equal width bars and spaces, with a fundamental period of 20 µm. If we use an FFT size of 64 points, Eq. **(7.62)** indicates that the size of the image patch for this lens is (64)(0.5 µm)/(4*0.05) = 160 µm. Thus, if we specify that the ideal image has 8 or more bars, the ideal image is effectively an infinite square wave, of period 20 µm. (The infinite periodicity is a result of using the FFT algorithm, which implicitly produces the output for one cycle of an infinite, periodic object.)

```
*OPERATING CONDITIONS: PARTIAL COHERENCE
   Effective source rad.:       --       Inner annular radius:        --
   X shift of source:           --       Y shift of source:           --
   X 1/e^2 of source:           --       Y 1/e^2 of source:           --
   Number of points in image:       64    Number of clear bars in image:    8
   Width of clear bar:        0.010000    Period of clear bars:      0.020000
   Irrad. between bars:         --       Phase between bars:          --
   Background irradiance:       --
   Normalization:    Object irradiance    Use equal image space incrmnts.:Off
```

We can now evaluate the in-focus images for both coherent and incoherent light. As expected, there is some ringing of the edges in the coherent image, while the incoherent images exhibits a decrease in modulation from the unit-modulation object. For an object period of p and wavelength λ_0, the Talbot distance is given by

$$d_{\text{Talbot}} = \frac{p^2}{\lambda_0} \tag{10.88}$$

In this case, the Talbot distance is $d_{\text{Talbot}} = (0.02\ \text{mm})^2/(0.0005\ \text{mm}) = 0.8$ mm. The coherent and incoherent images with focus shifts of 0.8 mm and 1.6 mm are shown below. In general, the coherent image replicates itself at integer multiples of the Talbot distance, and is also shifted laterally by one-half period if the integer is odd. With 0.8 mm of defocus, the incoherent image is virtually nonexistent (there are about 2 waves of defocus), but the coherent image is essentially identical to the in-focus image, except that it is shifted laterally by one-half of a period. If we examine the coherent image at two Talbot distances (1.6 mm) from focus, we see that the coherent image is the same as the nominal, in-focus image, while the incoherent image is gone.

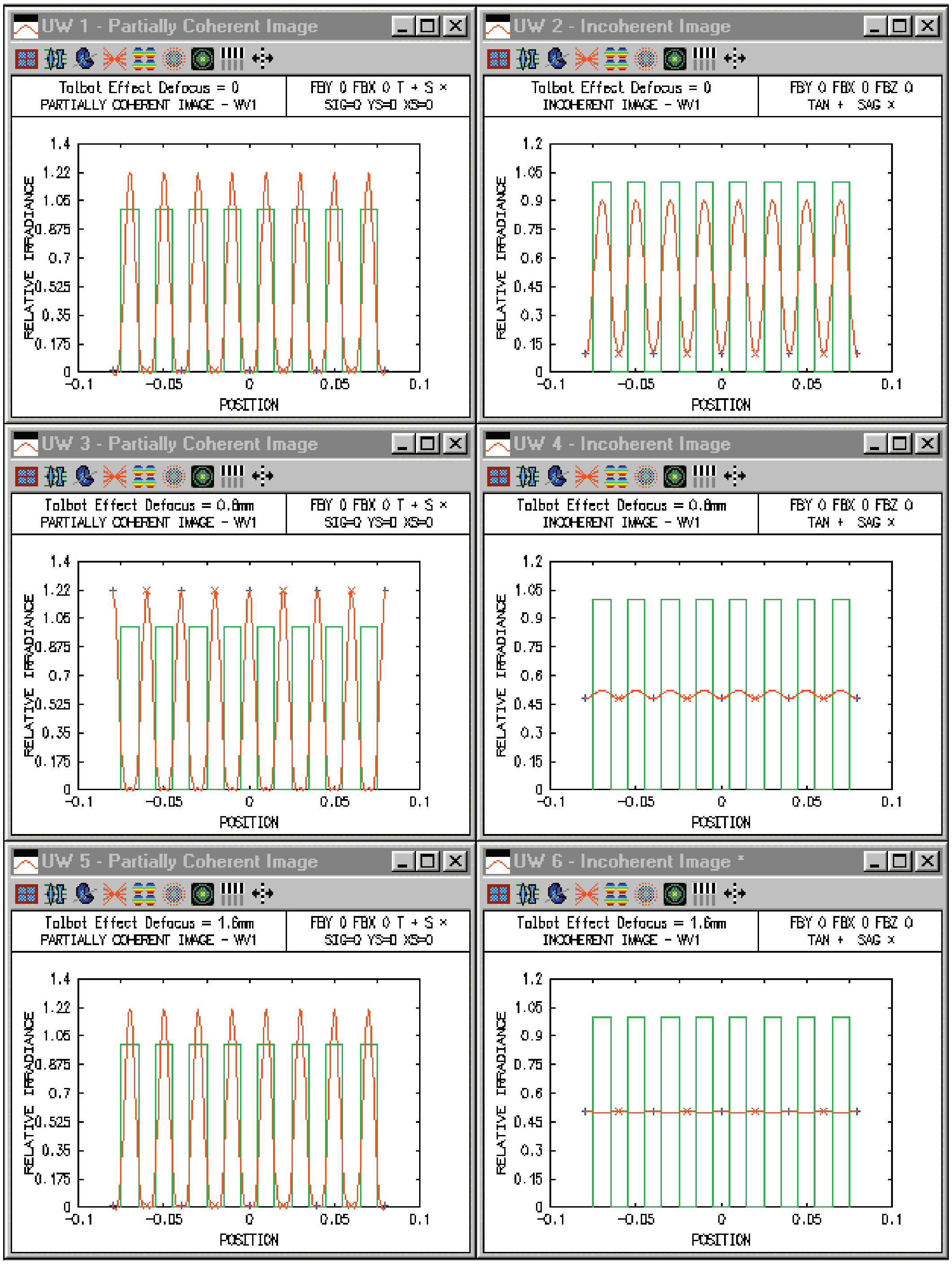

We can also examine the incoherent in-focus image of the square wave using the modulation transfer function. The image modulation of a square wave of frequency f_0 can be computed by resolving the square wave into its Fourier (i.e., sine wave) components and using the *MTF* value for each sine wave frequency. The resulting square wave modulation $S(f_0)$ is given by

$$S(f_0) = \frac{4}{\pi}\left[MTF(f_0) - \frac{1}{3}MTF(3f_0) + \frac{1}{5}MTF(5f_0) + \cdots \right] \qquad (10.89)$$

(Equation (10.89) can be found in, for example, Smith(11). For this lens, the cutoff frequency is 2 NA/λ_0 = 200 cycles/mm. Since our square wave has a frequency of f_0 = 1/0.02 mm = 50 cycles/mm, only the f_0 and $3f_0$ terms are non-zero in Eq. (10.89). We need to compute the on-axis *MTF* with a frequency increment of 50 cycles/mm. The number of aperture divisions in the spot diagram has been set to 32, so that the pupil sampling is the same as the partial coherence calculations.

```
*MODULATION TRANSFER FUNCTION Y
 WAVELENGTH 1
 NBR   FREQUENCY     MODULUS      PHASE              DIFF LIM MTF
  1       --        1.000000      --                   1.000000
  2    50.000000    0.684729      --                   0.684729
  3   100.000000    0.394089      --                   0.394089
  4   150.000000    0.147783      --                   0.147783
  5   200.000000      --          --                     --
CUTOFF FREQUENCY  193.654321
```

Using the above and Eq. (10.89), we find that the square wave modulation is S(50 cycles/mm) = $(4/\pi)(0.685 - 0.148/3) = 0.81$. To compare this with the output of the incoherent image calculation, we print out the incoherent image irradiance with an image plane increment of 0.01 mm, so that the minimum and maximum irradiance values are displayed.

```
*INCOHERENT IMAGE: MONOCHROMATIC
 WAVELENGTH 1
 NBR      Y       IRRADIANCE
  1   -0.080000    0.100449
  2   -0.070000    0.899551
  3   -0.060000    0.100449
  4   -0.050000    0.899551
  5   -0.040000    0.100449
  6   -0.030000    0.899551
  7   -0.020000    0.100449
  8   -0.010000    0.899551
  9      --        0.100449
 10    0.010000    0.899551
 11    0.020000    0.100449
 12    0.030000    0.899551
 13    0.040000    0.100449
 14    0.050000    0.899551
 15    0.060000    0.100449
 16    0.070000    0.899551
 17    0.080000    0.100449
```

Using the minimum (I_{min} = 0.100449) and maximum (I_{max} = 0.899551) irradiance values, the computed modulation is $S = (I_{max} - I_{min})/(I_{max} + I_{min}) = 0.80$, very close to the square wave modulation value given above, which was computed using a completely different technique.

11 W. J. Smith, *Modern Optical Engineering,* Second Edition, McGraw-Hill 1990, p. 355.